

Drag-Reducing Flows in Laminar-Turbulent Transition Region

Shu-Qing Yang

School of Civil, Mining
and Environmental Engineering,
Faculty of Engineering and Information Science,
University of Wollongong,
Northfields Avenue,
Wollongong, NSW 2522, Australia

Donghong Ding

School of Civil, Mining
and Environmental Engineering,
Faculty of Engineering and Information Science,
University of Wollongong,
Northfields Avenue,
Wollongong, NSW 2522, Australia

This study makes an attempt to investigate Newtonian/non-Newtonian pipe flows in a laminar-turbulent transition region, which is an extraordinarily complicated process and is not fully understood. The key characteristic of this region is its intermittent nature, i.e., the flow alternates in time between being laminar or turbulent in a certain range of Reynolds numbers. The physical nature of this intermittent flow can be aptly described with the aid of the intermittency factor γ , which is defined as that fraction of time during which the flow at a given position remains turbulent. Spriggs postulated that a weighting factor can be used to calculate the friction factor, applying its values in laminar and turbulent states. Based on these, a model is developed to empirically express the mean velocity and Reynolds shear stress in the transition region. It is found that the intermittency factor can be used as a weighting factor for calculating the flow structures in the transition region. Good agreements can be achieved between the calculations and experimental data available in the literature, indicating that the present model is acceptable to express the flow characteristics in the transition region. [DOI: 10.1115/1.4027455]

Keywords: drag reduction, polymer solution, transition region, turbulence structures, intermittency factor

1 Introduction

The process of a laminar flow becoming turbulent is known as laminar-turbulent transition. This is an extraordinarily complicated process that at present is not fully understood. Better understanding of this process may reveal the underlying nature of turbulence, which remains one of the unsolved problems in physics. As the result of many decades of intensive research, certain features have gradually become clear.

Osborne Reynolds [1] demonstrated the transition to turbulent flow in a classical experiment in which he examined an outlet from a large water tank through a small tube. When the water was slow, every fluid particle moves in parallel velocity along a straight path. When the speed increased, this orderly pattern of flow ceases to exist and strong mixing of all the particles occurs. This mixing process can be made visible with the aid of a thin thread of liquid dye into the pipe flow. The numerical value of the Reynolds number at which transition occurs (critical Reynolds number Re_{crit}) was established as being approximately at 2300 [2]. Accordingly, flows for which the Reynolds number $Re < Re_{crit}$ are supposed to be laminar, and the flows for which $Re > Re_{crit}$ are expected to be turbulent. The numerical value of the critical Reynolds number depends strongly on the conditions that prevail in the initial pipe length as well as in the approach to it [3–9]. Even Reynolds found that the transition occurred between $Re = 2000$ and 13,000, and he thought that the critical Reynolds number increases as the disturbances in the flow before the pipe are decreased. The critical Reynolds number has been observed in the range $1800 < Re_{crit} < 2300$ [10], and it can be delayed to 100,000 in carefully designed experiments [11]. The upper limit to which the critical Reynolds number can be driven if extreme care is taken to free the inlet from disturbances is not known at present. There exists, however, as demonstrated by numerous experiments, a lower bound for Re_{crit} , which is approximately at 2000 [2,11]. Normally, the lower bound for $Re_{crit} \approx 2300$ has been widely referred in the literature as “natural

transition” of Newtonian pipe flows [12,13]. For pipe flow with polymer additives, Draad et al. [6] reported that the large body of available literature on drag reduction shows no change in critical Reynolds number and the transition to turbulence for drag-reducing flows occurs at the same value as for Newtonian fluids, i.e., $Re = 2300$. Recently, Karami and Mowla [14] confirmed this value by observing that the turbulent flow occurs when Reynolds number exceeds 2300 in his experimental pipe lines with polymer additives. Below this value, the flow remains laminar, even in the presence of very strong disturbances. The current study makes attempt to investigate the flow structures in laminar-turbulent transition based on the assumption that the critical Reynolds number (the lower bound) is 2300. Since no plausible theoretical procedure exists for calculating the critical Reynolds number and the flow structures in laminar-turbulent transition, the formulae in this study are useful for fundamental research and practice. However, the empirical relationships used imply the presence of a basic underlying mechanism, the understanding of which might result in the formulation of a theoretical procedure.

In laminar flow, the longitudinal pressure gradient that drives the flow is proportional to the first power of the velocity, while in fully developed turbulent flow, the pressure gradient nearly becomes proportional to the square of the mean velocity of flow. Flow structures in both laminar flow and turbulent flow have been understood very well. However, no equation is available in the literature to describe the flow structures in the laminar-turbulent transition region. The key characteristic of this region is of its intermittent nature, which means that the flow alternates in time between being laminar or turbulent in a certain range of Reynolds numbers [2]. The physical nature of this intermittent flow can be aptly described with the aid of the intermittency factor γ , which is defined as that fraction of time during which the flow at a given position remains turbulent [15]. Hence, $\gamma = 1$ corresponds to continuous turbulent flow and $\gamma = 0$ denotes continuous laminar flow. Although it is obvious that γ depends on Reynolds numbers, the quantitative expression for this relationship is not available yet in the literature. The current study derives a formula to express the intermittency factor.

The addition of a minute amount of long-chain flexible polymer molecules to flowing fluids can drastically reduce turbulent

Contributed by the Fluids Engineering Division of ASME for publication in the JOURNAL OF FLUIDS ENGINEERING. Manuscript received January 22, 2013; final manuscript received April 13, 2014; published online July 24, 2014. Assoc. Editor: Mark F. Tachie.

friction, also known as drag reduction (DR), which was initially observed by Toms [16]. DR has subsequently attracted extensive research due to its practical applications and fundamental importance. Experiments [17–27] reveal that the existence of polymer additives can drastically reduce the turbulent drag and alter turbulent structures, including the turbulent velocity, the mean velocity, and Reynolds shear stress, etc. A comprehensive review of recent progress in understanding and predicting polymer drag reduction in turbulent wall-bounded shear flows can be found in White and Mungal [28].

For drag-reducing flows with polymer additives, one of the most important topics is the dynamic interactions between polymers and turbulence. To understand the interactions, it is necessary to investigate the drag-reducing flows in the laminar-turbulent transition region, because the drag reduction phenomenon disappears in laminar flow and it seems that the drag reduction only exists in the environment of turbulent eddies. For turbulent drag-reducing flows, previous investigations [29–33] show that the mean polymer shear stress can be expressed in analogy to eddy viscosity, i.e.,

$$\bar{\tau}_p = \rho \nu_{\text{eff}} \cdot \frac{d\bar{u}}{dy} = \rho \alpha_* u_* h \cdot \frac{d\bar{u}}{dy} \quad (1)$$

where α_* is the apparent viscoelasticity of the solution, ρ is the density of the solution, \bar{u} is the time-averaged velocity, ν_{eff} is the effective viscosity caused by polymers, u_* is the wall shear velocity, h is the flow depth or pipe radius, and y is the distance from the wall. It should be pointed out that, in the eddy diffusivity model, it is possible to assume that the distance from the wall y should be used to express the eddy viscosity that L'vov et al. [34] have extensively studied, while our research shows that h is a better parameter rather than y for describing the drag-reducing flows in our model.

According to the momentum conservation principle, the stress balance has the following form:

$$\bar{\tau}_p = \bar{\tau} - \left(\mu \frac{d\bar{u}}{dy} - \rho \overline{u'v'} \right) \quad (2)$$

where $\bar{\tau}$ is the total shear stress, μ is the dynamic viscosity of the solution, and $-\overline{u'v'}$ is the Reynolds shear stress.

By inserting Eq. (1) into Eq. (2), Yang and Dou [29,30] obtained the equation of drag-reducing flows in the fully developed turbulent state

$$\nu D_* \frac{d\bar{u}}{dy} - \overline{u'v'} = u_*^2 \left(1 - \frac{y}{h} \right) \quad (3)$$

where

$$D_* = 1 + \alpha_* \frac{u_* h}{\nu} \quad (4)$$

where ν is the kinetic viscosity of the solution and $u_* h / \nu (=R_*)$ is the friction Reynolds number.

Yang and Dou [31,32], hence, obtained equations of the velocity distribution and friction factor in Newtonian and drag-reducing turbulent flows. However, the structure of drag-reducing flows in laminar-turbulent transition is still not known.

The objectives of this paper are to: (1) derive the relationship between Reynolds number Re and the intermittency factor γ in the transition region, (2) analyze the velocity profiles in the laminar-turbulent transition region by introducing the weighting factor, (3) confirm the existence of the weighting factor using the data of friction factor, (4) express the velocity distribution in the

transition region, and (5) investigate turbulence structures in the transition region by applying the intermittency factor.

2 Intermittent Nature and Intermittency Factor in the Transition Region

Experiments [2] show that, in the transition region, turbulence is of intermittent nature, occurring at one moment and disappearing at another. If T denotes the total period of the observation time and T_t and T_l denotes the duration of turbulent and laminar flow, respectively, one has

$$T = T_t + T_l \quad (5)$$

If we define

$$\gamma_t = \frac{T_t}{T}, \quad \gamma_l = \frac{T_l}{T} \quad (6)$$

then one has

$$\bar{\gamma}_t = \lim_{T \rightarrow \infty} \frac{T_t}{T}, \quad \bar{\gamma}_l = \lim_{T \rightarrow \infty} \frac{T_l}{T} \quad (7)$$

where $\bar{\gamma}_t$ and $\bar{\gamma}_l$ represent the probabilities of occurrence of turbulent and laminar flows, respectively. By following the spot theory proposed by Emmons [35], Rotta [15] measured experimentally $\bar{\gamma}_t$ in the pipe inlet area using a hot wire anemometer; he found that this quantity is dependent upon both the Reynolds number and the measuring distance from the pipe entrance, and his results suggest that, for fully developed pipe flow, $\bar{\gamma}_t$ depends on Reynolds number only.

Substituting Eq. (7) into Eq. (5), one obtains

$$\bar{\gamma}_t + \bar{\gamma}_l = 1 \quad (8)$$

Then, Dou [36] obtained the following modeled equations for the relationship between the intermittency factor and Reynolds number (see Appendix):

$$\bar{\gamma}_t = \begin{cases} \frac{1}{e} \left[\sum_{n=1}^{\infty} \frac{n}{n!} \left(\frac{R_{\text{crit}^*}}{R_*} \right)^{2n} \right], & \text{for } R_* \geq R_{\text{crit}^*} \\ 1 & \text{for } R_* \leq R_{\text{crit}^*} \end{cases} \quad (9)$$

$$\bar{\gamma}_l = \begin{cases} 1 - \frac{1}{e} \left[\sum_{n=1}^{\infty} \frac{n}{n!} \left(\frac{R_{\text{crit}^*}}{R_*} \right)^{2n} \right], & \text{for } R_* \geq R_{\text{crit}^*} \\ 0 & \text{for } R_* \leq R_{\text{crit}^*} \end{cases} \quad (10)$$

where R_{crit^*} ($= u_{\text{crit}^*} h / \nu$) is the critical friction Reynolds number and u_{crit^*} is the critical wall shear velocity at the moment the flow becomes turbulent.

It should be stressed that the intermittency factor may be dependent on x , the distance from the pipe's entrance, but it is independent of y , the normal distance from a wall as observed by Rotta [15]. For the fully developed turbulent flow that the entrance effect is negligible, the intermittency factor should be independent of x ; thus, it is only a function of Reynolds number as shown in Eq. (10). In other words, one value of intermittency can be used to scale the entire profile.

For Newtonian fluid flow, the experiments show that, for a circular pipe, the critical Reynolds number $Re_{\text{crit}} = VD/\nu$ is approximately 2300, where V is the overall averaged velocity and D is the diameter of the pipe. Then, the relation between the critical Reynolds number and the critical friction Reynolds number is $R_{\text{crit}^*} = (2Re)^{0.5} = 67.82$ [31]. It should be stressed that the R_{crit^*} may be different from different researchers, and the value of that in drag-reducing flow may be different from that in Newtonian flow.

3 D_* and Reynolds Shear Stress in the Transition Region

Spriggs [37] was the previous researcher who addressed the significance of the intermittency factor as he argued “construction of a simple model of transition is possible by visualizing this region as being just a combination of laminar flow and turbulent flow. The intermittency factor is used as a weighting factor.” By following this idea, one can establish the expression of turbulent velocity in the transition region, i.e.,

$$\left(\sqrt{u'^2}\right)_{\text{transition}} = \bar{\gamma}_t \left(\sqrt{u'^2}\right)_{\text{turbulence}} \quad (11)$$

where u' is the fluctuation of axial velocity. In Eq. (11), the laminar term disappears as the velocity fluctuation in this region is zero. Likewise, Reynolds shear stress can be expressed by

$$\left(-\overline{u'v'}\right)_{\text{transition}} = -\overline{(\gamma_t u')(\gamma_t v')} = \bar{\gamma}_t^2 \left(-\overline{u'v'}\right)_{\text{turbulence}} \quad (12)$$

where v' is the fluctuation of the velocity in wall-normal direction. Equation (12) states that the Reynolds shear stress in the laminar-turbulent transition region is proportional to the square of the intermittency factor.

It is widely accepted [28,38] that the effect of polymer molecule stretching in a turbulent flow produces an increase in the effective viscosity and the large increase in the effective viscosity will suppress turbulent fluctuations, resulting in the suppression of the Reynolds shear stress. As D_* is the measurement of elastic parameter that is proportional to the turbulent velocities, one can postulate that $D_* > 1$ appears only in the period of turbulent flow in the transition region and it should be proportional to the square of the intermittency factor as the Reynolds shear stress in this region. Based on this argument, one can extend Eq. (4) into the following form:

$$D_* = 1 + \bar{\gamma}_t^2 \alpha_* \frac{u_* h}{\nu} \quad (13)$$

It is fairly clear that drag reduction occur only in turbulent status from Eq. (13), since $\bar{\gamma}_t^2 = 0$ in laminar status and D_* becomes 1, meaning no drag reduction occurs. This is a direct inference of the eddy diffusivity model, as Eq. (1) or Eq. (13) indicates that the eddy viscosity must become 0 or the drag reduction phenomenon will certainly disappear in laminar status. Equation (1) also demonstrates that the drag reduction is a near wall effect, as the velocity gradient has the maximum value in the boundary layer and reduces gradually when far from the wall.

4 The Velocity Profile and Friction Factor in the Transition Region

It is a well-documented fact that the flow in the transition region is laminar at one moment and becomes turbulent at another, and the interval of this alternation is unequal and irregular. Based on experimental observations, Schlichting [2] inferred that the velocity profile in the transition region is sometimes corresponding to laminar distribution while sometimes to turbulent one. Therefore, it is fairly reasonable to express the velocity distribution in the transition region as the following form:

$$\frac{\bar{u}}{u_*} = \bar{\gamma}_t \beta \frac{\bar{u}_t}{u_{*t}} + \bar{\gamma}_l \beta_1 \frac{\bar{u}_l}{u_{*l}} \quad (14)$$

where the subscripts of “ t ” and “ l ” denote turbulent and laminar states, respectively; $\beta = u_{*l}/u_*$, $\beta_1 = u_{*t}/u_*$, u_{*t} , and u_{*l} are the shear velocities during the laminar and turbulent states.

In laminar flow, the Reynolds shear stress is 0. Hence, the integration of Eq. (3) with respect to y yields

$$\frac{\bar{u}_l}{u_{*l}} = \frac{u_{*l} y}{\nu D_*} \left(1 - \frac{y}{2h}\right) \quad (15)$$

For a channel flow [39,40] and a pipe flow, Yang and Dou [30] obtained the following equation for the velocity distribution in the fully developed turbulent flows:

$$\frac{\bar{u}_t}{u_{*t}} = 2.5 \ln \left(1 + \frac{u_{*l} y}{5\nu D_*}\right) + (5.8D_*^2 + 1.25) \left(\frac{\frac{u_{*l} y}{5\nu D_*}}{1 + \frac{u_{*l} y}{5\nu D_*}}\right)^2 + 2.5 \frac{\frac{u_{*l} y}{5\nu D_*}}{1 + \frac{u_{*l} y}{5\nu D_*}} \quad (16)$$

As the first approximation, we assume $u_{*t} \approx u_{*l} \approx u_*$ or $\beta = \beta_1 = 1$. Inserting Eqs. (15) and (16) into Eq. (14), one can obtain the velocity distribution in the laminar-turbulent transition region

$$\frac{\bar{u}}{u_*} = \bar{\gamma}_t \left[2.5 \ln \left(1 + \frac{u_* y}{5\nu D_*}\right) + (5.8D_*^2 + 1.25) \left(\frac{\frac{u_* y}{5\nu D_*}}{1 + \frac{u_* y}{5\nu D_*}}\right)^2 + 2.5 \frac{\frac{u_* y}{5\nu D_*}}{1 + \frac{u_* y}{5\nu D_*}} \right] + \bar{\gamma}_l \left[\frac{u_* y}{\nu D_*} \left(1 - \frac{y}{2h}\right) \right] \quad (17)$$

If $D_* = 1$, it gives the velocity distribution in Newtonian fluid flows; otherwise, it represents the velocity profiles in drag-reducing flows.

The overall averaged velocity V can be obtained by integrating Eq. (17) and has the following form:

$$\frac{V}{u_*} = \bar{\gamma}_t \left[\left(2.5 - \frac{23.2D_*^2 + 5}{R_*/(5D_*)} - \frac{34.8D_*^2 + 10}{(R_*/5/D_*)^2}\right) \ln \left(1 + \frac{R_*}{5D_*}\right) + 5.8D_*^2 + \frac{34.8D_*^2 + 10}{R_*/(5D_*)} \right] + \bar{\gamma}_l \frac{R_*}{4D_*} \quad (18)$$

The friction factor is defined by

$$f = \frac{2}{\left(\frac{V}{u_*}\right)^2} \quad (19)$$

Inserting Eq. (18) into Eq. (19), one can obtain the formula of the friction factor of Newtonian/drag-reducing flows from laminar flow to turbulent flow, as well as the laminar-turbulent transition flow. If $\bar{\gamma}_t = 0$ or $\bar{\gamma}_l = 1$, Eq. (19) gives the friction factor of laminar flow; else if $\bar{\gamma}_t = 1$ or $\bar{\gamma}_l = 0$, it gives the friction factor of fully developed turbulent flow. Otherwise, it could give the friction factor of laminar-turbulent transition flow.

It should be stressed that, different from Eq. (19), Spriggs [37] proposed that the friction factor in the transition region can be expressed as

$$f = (1 - \bar{\gamma}_t) f_{\text{laminar}} + \bar{\gamma}_t f_{\text{turbulent}} \quad (20)$$

Equation (19) is more physically reasonable, since the friction factor is proportional to the square of the velocity, and the current study starts from Eq. (14), in which the velocities in the same direction are linearly summable.

For Newtonian fluid flow ($D_* = 1$), given friction Reynolds number R_* , one can estimate $\bar{\gamma}_t$ by using Eq. (10), and then the friction factor can be calculated by applying Eqs. (18) and (19). For drag-reducing flows, once α_* is determined, one can calculate

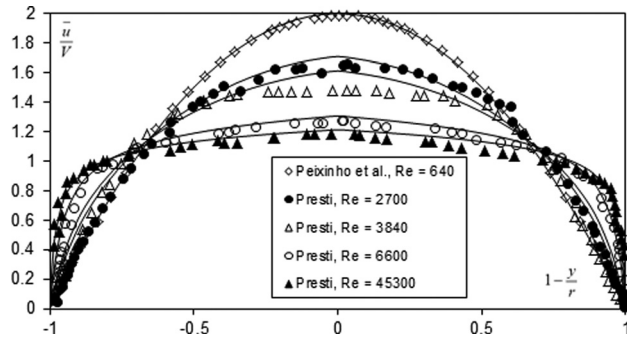


Fig. 1 Measured (symbols) and calculated (lines) velocity profiles in laminar, transition, and turbulent flow regions. For $Re = 640$, glucose syrup, $\bar{\gamma}_t = 0$ and $D_* = 1$; for $Re = 2700$, 0.4% CMC, $\bar{\gamma}_t = 0.75$ and $D_* = 1.03$; for $Re = 3840$, 0.2% PAA, $\bar{\gamma}_t = 0.85$ and $D_* = 1.09$; for $Re = 6600$, 0.14% Carbopol 934, $\bar{\gamma}_t = 0.99$ and $D_* = 1.29$; and for $Re = 45,300$, 0.09% CMC/0.09% XG, $\bar{\gamma}_t = 1$ and $D_* = 1.56$.

the value of D_* and then determine the friction factor similar to Newtonian fluid flows. However, the apparent viscoelasticity α_* of the solution is unknown at first; one needs to adjust it to yield the best agreement between the measured data and predictions of the velocity distribution or friction factor. The values of α_* listed in Figs. 4 and 5 are determined by using the later method.

5 Verification of the Velocity Distribution and Friction Factor

This study established the model for calculating the velocity distribution and friction factor of drag-reducing flows in the laminar-turbulent transition region. It is important to test the model by comparing the predictions with experimental data available in the literature. The current model is based on two assumptions: (1) Eq. (14) that the velocity in the transition region is a combination of laminar and turbulent velocities by adjusting the weighting factor and (2) Eq. (10) that the calculation of the intermittency factor is made by applying the friction Reynolds number and the critical friction Reynolds number.

Firstly, the authors test assumption 1. Presti [41] in Escudier et al. [42] measured the velocity profiles in a 50 mm diameter UPVC pipe system. Laser-Doppler anemometry was used to measure the point velocity in the pipe. Different polymers were used, such as carboxymethylcellulose (CMC), xanthan gum (XG), and polyacrylamide (Separant AP 273 or PAA). Figure 1 shows the comparison of measured and calculated velocity profiles in the pipe flow; the symbols are the experimental data collected by Presti [41], and Reynolds number, polymer type, and concentration are listed in the caption. Equation (13) is used to calculate D_* , in which α_* is obtained from the measured friction factor. It can be seen that, from laminar flow to turbulent flow, the velocity profiles gradually change from the parabolic curve to the logarithmic type. By adjusting the weighting factor, Eq. (14) can capture the majority of the measured velocity profiles. Good agreement supports the validity of the assumption in Eq. (14).

Secondly, one needs to examine whether Eq. (10) is valid or not. On one hand, using experimental data of the friction factor in the transition region, one can calculate the intermittency factor by using Eq. (18). On the other hand, the intermittency factor can be calculated directly by applying Eq. (10). Through comparing the intermittency factor obtained from two ways, one can verify easily whether Eq. (10) is valid or not. Virk [17] systematically measured the flow resistance in a smooth pipe with Newtonian and non-Newtonian fluids, which are available for the current study. Virk measured the friction factor in a smooth pipe by increasing the flow rate, and he used polyethyleneoxide N750 as the additive with its concentrations of 43.6 ppm and 98.6 ppm. The elastic

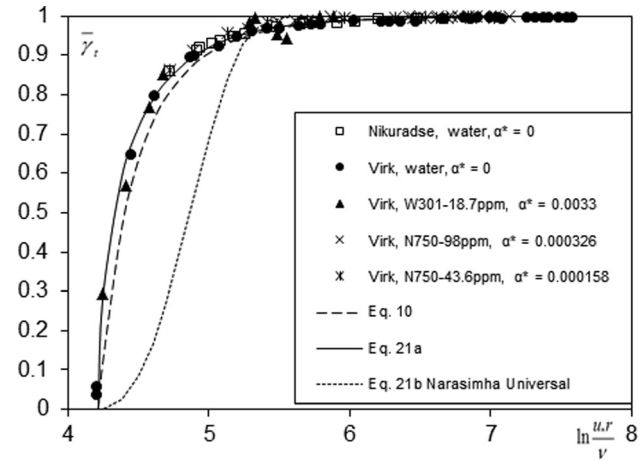


Fig. 2 Comparison of weighting factor determined from the measured friction factor with the intermittency factor, i.e., Eq. (10) and its modified form Eq. (21)

factors α_* are found to be 0.000158 and 0.000326 [32], respectively. He also used polyethyleneoxide W301 with a concentration of 18.7 ppm, which yields $\alpha_* = 0.0033$. All obtained intermittency factor are presented in Fig. 2. For comparison, Eq. (10), which was developed by Dou, is also included, in which $R_{*crit} = 67.82$ is used in the calculation. It is surprising to see that all data points from different sources are consistent and Eq. (10) can express the tendency, and a simpler and better form is given in Eq. (21) as

$$\bar{\gamma}_t = \left[1 - \left(\frac{\ln R_{*k}}{\ln R_*} \right)^{11} \right]^{0.5} \quad (21a)$$

The intermittency in the boundary layer flows and, in the early stages of pipe transition, has been investigated by many researchers [43–45]. Their results show that the intermittency factor depends on both streamwise distance and pipe Reynolds number, and it is often assumed that, if the pipe is sufficiently long, the intermittent pattern may be replaced by nearly periodic oscillations. Figure 2 shows that the assumption may not be correct, as in a very long pipe, the intermittency factor depends on the Reynolds number only (independent of streamwise distance). The universal distribution proposed by Narasimha [45] has the following form:

$$\bar{\gamma}_t = 1 - \exp(-4.12\xi^2) \quad (21b)$$

where $\xi = (x - x_r)/\lambda$, $\lambda = x(\gamma = 0.75) - x(\gamma = 0.25)$, x is the streamwise distance, and x_r is the distance where spots are born. Equation (21b) indicates that, for a pipe flow, if x or ξ approaches infinity, one obtains $\bar{\gamma}_t = 1$. In other words, it indicates that the laminar state will eventually disappear no matter how small the Reynolds number is. This seems unreasonable. If we define $\xi = (R_* - R_{*k})/R_{*k}$, the result is shown in Fig. 2 and the function cannot match the data well no matter how we define λ . This indicates that the knowledge developed from the boundary layer flows and pipe entrance flow cannot be extended to the fully developed pipe flow directly.

Figure 2 shows that the intermittency factor obtained from Eq. (18) is identical to its value from Eq. (10), which indicates that Eq. (10) is valid and the formula Eq. (21) can be used to estimate the intermittency factor by applying the critical friction Reynolds number and the friction Reynolds number. It can be seen from Fig. 2 that Eq. (10) underestimates slightly the intermittency factor in the region of $\ln(u_* r / \nu) < 4.9$; this may be caused by imperfect facilities, as only nine data points exist, or the imperfect theory that considers only the pure statistical properties

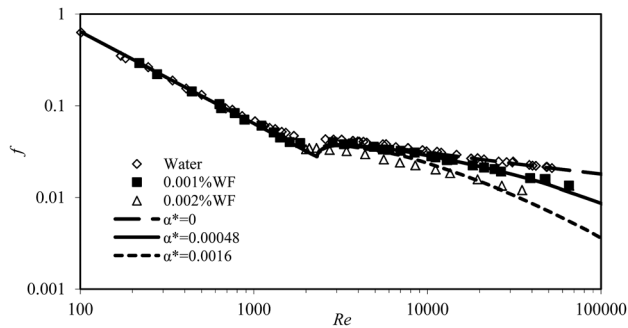


Fig. 3

Fig. 3 Friction factor versus Reynolds number in laminar-turbulent transition region based on Wójs's experimental data [46]

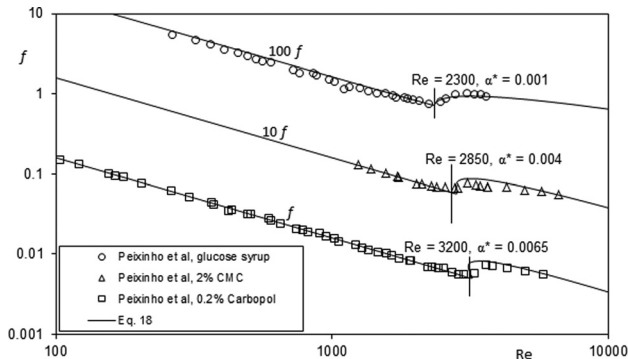


Fig. 4 Friction factor versus Reynolds number based on Peixinho et al.'s [47] measurements

without consideration of dynamic properties. It can be inferred that the effect of polymer additives has no influence on the intermittency factor. This is consistent with Virk's observation [19] that "the onset of drag reduction occurs at the same wall shear stress which is essentially independent of polymer concentration." Therefore, one can conclude that the existence of polymer would not change the critical Reynolds number and the intermittency factor in the transition region.

It can be seen from any measured $f \sim Re$ diagram that the appearance of the first turbulent patch in a fluid corresponds closely to deviation from laminar flow relation, and the Reynolds number at this point is referred as the critical Reynolds number in the current study. As mentioned, the critical Reynolds number may be different from 2300; thus, it is worthwhile to investigate the influence of the critical Reynolds number on the predictability of friction factor. For this purpose, Wójs [46] measured the friction factor in a smooth pipe from laminar, the transition to fully developed turbulent regions. Polyacrylamide Rokrysol was used in his experiments, and polymer concentrations were 0.001% and 0.002%. Figure 3 shows that the critical Reynolds number is about 2800. The apparent viscoelasticity of the solutions $\alpha_* = 0.00048$ and 0.0016 are obtained for the concentrations of 0.001% and 0.002%, respectively. The calculated friction factors using the critical Reynolds number (2800) are included in Fig. 3, and it can be seen that good agreement is achieved.

Peixinho et al. [47] carefully observed the critical Reynolds number and its impact on friction factor, and their results are shown in Fig. 4, in which the solid lines are calculated results using Eq. (18). It can be seen that the critical Reynolds number varies from 2300 to 3200, and the corresponding $R_{crit*} = 67.82$, 75.5, and 80, respectively. The apparent viscoelasticity α_* is obtained by fitting the data points. It can be seen that the model

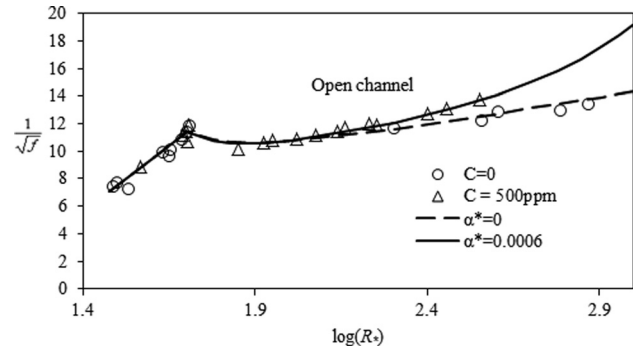


Fig. 5 Friction factor versus Reynolds number in laminar-turbulent transition region based on Dou and Wang's [48] measurements

proposed in this study can express well the friction factor at various critical Reynolds numbers.

To show the current model is also valid for channel flows, Dou and Wang's [48] experimental data is used, in which they measured friction factor in a smooth open channel, and the results are shown in Fig. 5. In Fig. 5, C is the polymer concentration and lines are the calculated results using Eq. (18). It can be seen that the predictions provide satisfactory agreement, indicating that the current model is acceptable for prediction of friction factor in channel flows for both Newtonian and non-Newtonian fluids.

6 Turbulence Structures

As the intermittency factor is one of the convenient and also the most important characteristics of the transition region, it would be interesting to investigate how the intermittency factor affects the turbulent structures in the transition region. For fully developed turbulent flows, Yang and Dou [30] expressed the turbulent velocity fluctuations as follows:

$$\overline{u'v'} = -\frac{U^2 T_1}{2} \frac{d\bar{u}}{dy} + \left(\frac{mL^2}{4} - \frac{m^2 L^2}{8}\right) \left(\frac{d\bar{u}}{dy}\right)^2 \quad (22)$$

and the mean square of the velocity fluctuations in streamwise and wall-normal directions can be expressed as

$$\overline{u'^2} = \frac{U^2}{2} + \frac{9}{4} m^2 L^2 \left(\frac{d\bar{u}}{dy}\right)^2 \quad (23)$$

$$\overline{v'^2} = \frac{U^2}{2} + \frac{1}{4} m^2 L^2 \left(\frac{d\bar{u}}{dy}\right)^2 \quad (24)$$

where U , T , and L represent the eddy's characteristic velocity, time, and length, respectively; m is introduced to consider the damping effect of wall on the eddy size. The eddy's characteristics are determined by its location, i.e., vertical distance y , thickness of viscous sublayer δ , local shear stress τ , and boundary shear stress τ_* ; the following criteria of similarity were used:

$$m = \frac{y}{\delta}; \quad U = u_* \sqrt{\frac{y}{\delta + y}}; \quad L = \kappa \delta \sqrt{1 - \frac{y}{h}}; \quad T_1 = \kappa \left(1 - \frac{y}{h}\right) \frac{\delta + y}{u_*} \quad (25)$$

in which κ is the Karman constant 0.4, δ is the thickness of viscous sublayer, and $u_* \delta / \nu = 11.6 D_*^3$.

By substituting the expression of Reynolds shear stress in turbulence into Eq. (12), one obtains the following equation:

$$\left(-\frac{\overline{u'v'}}{u_*^2}\right)_{tr} = -\overline{\gamma}_t \cdot \left\{ \left(1 - \frac{y}{h}\right) - \frac{1 - \frac{y}{h}}{1 + \left(1 - \frac{y}{h}\right) \frac{u_* y}{5\nu D_*}} - \frac{\left[0.464 D_*^2 \left(\frac{u_* y}{\nu D_*}\right) - 0.02 \left(\frac{u_* y}{\nu D_*}\right)^2\right] \left(1 - \frac{y}{h}\right)^3}{\left[1 + \left(1 - \frac{y}{h}\right) \frac{u_* y}{5\nu D_*}\right]^3} \right\} \quad (26)$$

where the subscript “tr” denotes transition regime. Similar to Eq. (24), the intensities of turbulent velocity in the laminar-turbulent transition region can be expressed as follows:

$$\left(\frac{\sqrt{v'^2}}{u_*}\right)_{tr} = \overline{\gamma}_t \left[\frac{\frac{u_* y}{\nu D_*}}{23.2 D_*^2 + 2 \frac{u_* y}{\nu D_*}} + 0.04 \left(1 - \frac{y}{h}\right) \left(\frac{y}{u_*} \frac{d\overline{u}}{dy}\right)^2 \right]^{1/2} \quad (27)$$

$$\left(\frac{\sqrt{u'^2}}{u_*}\right)_{tr} = \overline{\gamma}_t \left[\frac{\frac{u_* y}{\nu D_*}}{23.2 D_*^2 + 2 \frac{u_* y}{\nu D_*}} + 0.36 m_o \left(1 - \frac{y}{h}\right) \left(\frac{y}{u_*} \frac{d\overline{u}}{dy}\right)^2 \right]^{1/2} \quad (28)$$

where

$$\frac{y}{u_*} \frac{d\overline{u}}{dy} = \frac{\frac{u_* y}{\nu D_*}}{1 + \frac{u_* y}{5\nu D_*}} + 0.02 \frac{23.2 D_*^2 \left(\frac{u_* y}{\nu D_*}\right)^2 - \left(\frac{u_* y}{\nu D_*}\right)^3}{\left(1 + \frac{u_* y}{5\nu D_*}\right)^3} \quad (29)$$

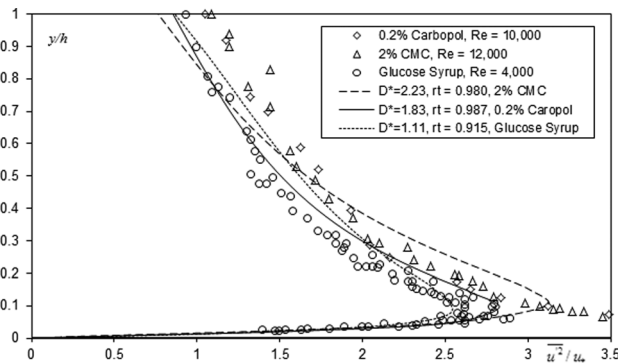


Fig. 6 Turbulent intensity profiles measured by Peixinho et al. [47] and its comparison with Eq. (28)

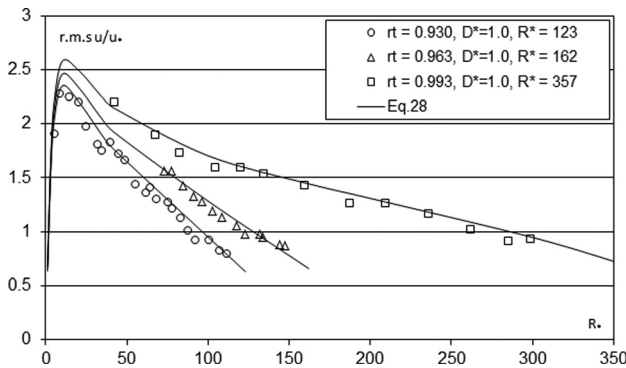


Fig. 7 Distribution of measured rms of streamwise velocity fluctuations in the laminar-turbulent transition region of Newtonian fluid flow

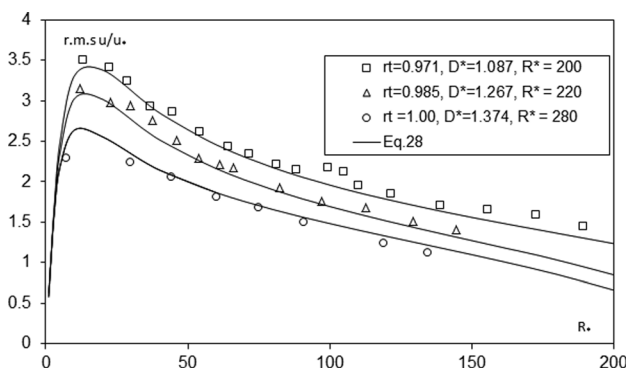


Fig. 8 Distribution of measured rms of streamwise velocity fluctuations in the laminar-turbulent transition region of drag-reducing flow

where m_o is included to express the large drag reduction (LDR) effect [30]. For Newtonian and small drag reduction (SDR), $m_o = 1$, i.e., no correction is needed.

In the literature, no measured Reynolds shear stress in the transition region is available; thus, Eq. (26) cannot be verified by experimental data. Peixinho et al. [47] measured the turbulent intensity profiles of drag-reducing flows, and their experimental results are shown in Fig. 6, in which Eq. (28) is also included for comparison. The calculated results are presented by solid lines. The intermittency factor is calculated based on Reynolds number; $\overline{\gamma}_t$ and α_* shown in Fig. 4 were used to determine D_* . The correction parameter m_o for glucose syrup, CMC, and Carbopol are 1, 0.45, and 0.3, respectively. Although the data points and the lines are scattered, careful look shows that, for SDR, i.e., glucose syrup, the agreement between measured and calculated turbulent intensity profiles is acceptable relative to other methods, like numerical models [49].

Figures 7 and 8 show the rms of streamwise velocity fluctuations in Newtonian fluid flow and drag-reducing flow in open channels measured by Dou and Wang [48], in which $\overline{\gamma}_t$ and D_* are determined using Eqs. (21) and (13), respectively. The turbulent velocity fluctuations calculated from Eq. (28) are also included.

It can be seen from Figs. 6–8 that Eq. (28) is valid to express the turbulent intensity in the transition region. It is valid for both Newtonian fluid flow and LDR flows $m_o = 1$, but for LDR, Eq. (28) needs a modification as in the fully turbulent region.

7 Conclusion

This study investigates the flow characteristics of Newtonian/non-Newtonian fluid flows in the laminar-turbulent transition region. The study confirms Spriggs’ [37] intuition that “construction of a simple model of transition is possible by visualizing this regime as being just a combination of laminar flow and turbulent flow. The intermittency factor can be empirically used as a weighting factor.” However, this is achievable only when the velocities in the two regions are combined, rather than friction factor, as proposed by Spriggs [37]. The equations of time-averaged velocity, friction factor, Reynolds shear stress, and turbulent velocity fluctuations developed by the authors have been

extended to the transition region. These equations are fairly consistent with the available data over a range of conditions, and the following conclusions can be drawn:

- (1) The weighting factor has been obtained from the measured friction factors, and it is confirmed that the weighting factor can be quantitatively predicted by Eq. (10) or simplified Eq. (21), which are developed to express the intermittency factor. This agreement implies that the weighting factor is identical to the intermittency factor. More experiments are needed in the future to check this conclusion by measuring the velocity in the transition region.
- (2) Under natural conditions, for Newtonian/drag-reducing fluid flow, 2300 can be roughly used as the critical Reynolds number in pipes. However, this model is still valid to express the flow characteristics in the transition region when the critical Reynolds number is various.
- (3) From laminar state to fully developed turbulent state with the increase of Reynolds number, the velocity profile in a pipe flow gradually deforms from parabolic to logarithmic curves. By adjusting the weighting factor, the combination model can capture well this characteristic.
- (4) The present model can express the turbulent intensity well in Newtonian fluid flow and SDR flow, but it needs to be modified for predicting the turbulent intensity in LDR flow.

Acknowledgment

The work is supported, in part, by National Science Foundation of China (51228901 and 51239001).

Nomenclature

D = diameter of the pipe
 $D_* = 1 + \alpha_*(u_*h/\nu)$
 f = friction factor
 h = flow depth or pipe radius
 L = eddy's characteristic length
 m = a number to consider the damping effect of wall
 m_0 = coefficient to express the effect of large drag reduction
 $R_* = u_*h/\nu$, friction Reynolds number
 Re = Reynolds number
 Re_{crit} = critical Reynolds number
 T = total period of the observation time
 T_1 = eddy's characteristic velocity, time
 T_l = duration of laminar flow
 T_t = duration of turbulent status
 u_{crit*} = critical wall shear velocity
 u_* = wall shear velocity
 u' = fluctuation of axial velocity
 $-u'v'$ = Reynolds shear stress
 \bar{u} = the time-averaged velocity
 U = eddy's characteristic velocity
 v' = fluctuation of the velocity in wall-normal direction
 V = overall averaged velocity
 x = streamwise distance
 x_t = the distance where spots are born
 y = distance from the wall
 α_* = apparent viscoelasticity of the solution
 $\bar{\gamma}_l$ = probabilities of laminar flows, respectively
 $\bar{\gamma}_t$ = probabilities of occurrence of turbulent flow
 δ = thickness of viscous sublayer
 κ = Karman constant, 0.4
 λ = a characteristic distance in x -direction
 μ = dynamic viscosity of the solution
 ν = kinetic viscosity of the solution
 ν_{eff} = the effective viscosity caused by polymers
 $\xi = (x - x_t)/\lambda$
 ρ = density of the solution
 τ = shear stress

τ_* = boundary shear stress
 $\bar{\tau}$ = total shear stress

Subscripts

l = laminar state
 t = turbulent state
 tr = transition regime

Appendix: Determination of the Intermittency Factor

Experiments [2] show that, in the transitional region, turbulence is of an intermittent nature, occurring at one moment and disappearing at another. Rotta [15] observed the transition flow in pipes with hot-wire anemometer, and it was found that the flow is laminar at one moment and turbulent at another. Experiments also show that the interval of alternation between the laminar and the turbulent is unequal and irregular and the duration of the turbulence is sometimes long and sometimes short. The frequency of the interchange between the laminar and the turbulent also is undeterminable. So the phenomena observed in the transition state are of a pronounced stochastic character. If we let T denote the total period of observation, T_t the duration of turbulent flow, and T_l the duration of laminar flow, one can write

$$T = T_t + T_l \quad (A1)$$

we define

$$\gamma_t = \frac{T_t}{T}, \quad \gamma_l = \frac{T_l}{T} \quad (A2)$$

and then we have

$$\bar{\gamma}_t = \lim_{T \rightarrow \infty} \frac{T_t}{T}, \quad \bar{\gamma}_l = \lim_{T \rightarrow \infty} \frac{T_l}{T} \quad (A3)$$

where $\bar{\gamma}_t$ and $\bar{\gamma}_l$ are the probabilities of occurrence of turbulent and laminar flows, respectively. And we have

$$\bar{\gamma}_t + \bar{\gamma}_l = 1 \quad (A4)$$

If we divide the period of observation into m small intervals of Δt , one has

$$T = m\Delta t \quad (A5)$$

As mentioned above, in the period of observation, the turbulent and the laminar would be interchanged and the duration of their appearance would be sometimes long and sometimes short. If K_1 is the times of turbulence occurrence with the duration equal to $1\Delta t$, K_2 is the times of turbulence occurrence with the duration equal to $2\Delta t$, and K_n is the times of turbulence occurrence with the duration equal to $n\Delta t$, one can write

$$T_t = K_1\Delta t + K_2(2\Delta t) + \dots + K_n(n\Delta t) = \Delta t \sum nK_n \quad (A6)$$

If there is a turbulence, the duration of which is equal to $n\Delta t$, and its permutation number relative to the duration of $1\Delta t$ and to the observation time with $1\Delta t$ is denoted by k_n , then the total permutation number of this turbulence in the period of observation $T = m\Delta t$ would be mnk_n . On the other hand, if the turbulence having the duration equal to $n\Delta t$ consists of n unit intervals and there are $n!$ different permutations, the total number of permutations of this turbulence occurring in the period of observation should be $K_n n!$. Therefore, one obtains

$$K_n = \frac{mn}{n!} k_n \quad (A7)$$

Substituting Eq. (A6) into Eq. (A7) and dividing it by T , one obtains

$$\gamma_t = \sum_{n=1}^m \frac{n^2}{n!} k_n \quad (\text{A8})$$

$$\bar{\gamma}_t = \lim_{m \rightarrow \infty} \sum_{n=1}^m \frac{n^2}{n!} k_n = \sum_{n=1}^{\infty} \frac{n^2}{n!} k_n \quad (\text{A9})$$

where \bar{k}_n is the statistic mean value of k_n . Under given flow conditions, it would be a stable value; in a general case, this value should be the function of the ratio of the Reynolds number R_* ($=u_*h/\nu$) to its critical value, at which the turbulent flow transits to laminar one. With the increase of the Reynolds number, the value of \bar{k}_n would be increased, but the increasing rate is generally decreased to make \bar{k}_n approach to its maximum value. Therefore, the derivative of \bar{k}_n , with respect to R_* ($=u_*h/\nu$), could be taken as the function of R_{*k}/R_* , i.e.,

$$\frac{d\bar{k}_n}{dR_*} = f\left(\frac{R_{*k}}{R_*}\right) \quad (\text{A10})$$

Assuming that this function can be expressed as a series in uneven powers, one can write

$$\frac{d\bar{k}_n}{dR_*} = \alpha \left(\frac{R_{*k}}{R_*}\right)^{2n+1} \quad (\text{A11})$$

where α is a coefficient of proportionality. The integration of Eq. (A11) gives

$$\bar{k}_n = -\frac{\alpha R_{*k}}{2n} \left(\frac{R_{*k}}{R_*}\right)^{2n} + C_1 \quad (\text{A12})$$

where C_1 is the constant of integration. When the Reynolds number is smaller than or equal to its critical value, the flow would be in a completely laminar state; consequently, no turbulence would occur. This boundary condition gives

$$C_1 = \frac{\alpha R_{*k}}{2n} \quad (\text{A13})$$

Inserting Eqs. (A12) and (A13) into Eq. (A9), we have

$$\bar{\gamma}_t = \frac{1}{2} \alpha R_{*k} \left(\sum_{n=1}^m \frac{n}{n!} \right) - \frac{1}{2} \alpha R_{*k} \left[\sum_{n=1}^m \frac{n}{n!} \left(\frac{R_{*k}}{R_*}\right)^{2n} \right] \quad (\text{A14})$$

When the Reynolds number is large enough, the flow would be in the turbulent state. Therefore, when $R_* \rightarrow \infty$, $\bar{\gamma}_t = 1$. Then, we have

$$\frac{1}{2} \alpha R_{*k} \left(\sum_{n=1}^{\infty} \frac{n}{n!} \right) = 1 \quad (\text{A15})$$

$$\alpha = \frac{2}{R_{*k} \left(\sum_{n=1}^{\infty} \frac{n}{n!} \right)} \quad (\text{A16})$$

Note that $\sum_{n=1}^{\infty} (n/n!) = e$, substituting Eq. (A15) into Eq. (A16), one obtains

$$\bar{\gamma}_t = \begin{cases} 1 - \frac{1}{e} \left[\sum_{n=1}^{\infty} \frac{n}{n!} \left(\frac{R_{*k}}{R_*}\right)^{2n} \right] & R_* \geq R_{*k} \\ 0 & R_* < R_{*k} \end{cases} \quad (\text{A17})$$

$$\bar{\gamma}_t = \begin{cases} \frac{1}{e} \left[\sum_{n=1}^{\infty} \frac{n}{n!} \left(\frac{R_{*k}}{R_*}\right)^{2n} \right] & R_* \geq R_{*k} \\ 1 & R_* < R_{*k} \end{cases} \quad (\text{A18})$$

For Newtonian fluid flow, the experiments show that, for a circular pipe, the critical Reynolds number $Re = VD/\nu$ is about 2300, where V is the mean cross-sectional velocity and D is the diameter of pipe. Then, the relation between the two critical Reynolds number is $R_* = (2Re)^{0.5} = 67.82$.

References

- Reynolds, O., 1883, "An Experimental Investigation of the Circumstances Which Determine Whether the Motion of Water Shall Be Direct or Sinuous, and of the Law of Resistance in Parallel Channels," *Proc. R. Soc. London*, **35**(224–226), pp. 84–99.
- Schlichting, H., 1979, *Boundary Layer Theory*, McGraw-Hill, New York, p. 452.
- Wyganski, I., and Champagne, F., 1973, "On Transition in a Pipe. Part I. The Origin of Puffs and Slugs and the Flow in a Turbulent Slug," *J. Fluid Mech.*, **59**(02), pp. 281–335.
- Wyganski, I. J., Sokolov, M., and Friedman, D., 1975, "On Transition in a Pipe. Part 2. The Equilibrium Puff," *J. Fluid Mech.*, **69**(02), pp. 283–304.
- Darbyshire, A., and Mullin, T., 1995, "Transition to Turbulence in Constant-Mass-Flux Pipe Flow," *J. Fluid Mech.*, **289**, pp. 83–114.
- Draad, A. A., Kuiken, G., and Nieuwstadt, F., 1998, "Laminar–Turbulent Transition in Pipe Flow for Newtonian and Non-Newtonian Fluids," *J. Fluid Mech.*, **377**, pp. 267–312.
- Eliahou, S., Tumin, A., and Wygnanski, I., 1998, "Laminar–Turbulent Transition in Poiseuille Pipe Flow Subjected to Periodic Perturbation Emanating From the Wall," *J. Fluid Mech.*, **361**, pp. 333–349.
- Hof, B., Juel, A., and Mullin, T., 2003, "Scaling of the Turbulence Transition Threshold in a Pipe," *Phys. Rev. Lett.*, **91**(24), p. 244502.
- Han, G., Tumin, A., and Wygnanski, I., 2000, "Laminar–Turbulent Transition in Poiseuille Pipe Flow Subjected to Periodic Perturbation Emanating From the Wall. Part 2. Late Stage of Transition," *J. Fluid Mech.*, **419**, pp. 1–27.
- Ben-Dov, G., and Cohen, J., 2007, "Critical Reynolds Number for a Natural Turbulence in Pipe Flows," *Phys. Rev. Lett.*, **98**(6), p. 064503.
- Hof, B., van Doorne, C. W., Westerweel, J., Nieuwstadt, F. T., Faisst, H., Eckhardt, B., Wedin, H., Kerswell, R. R., and Waleffe, F., 2004, "Experimental Observation of Nonlinear Traveling Waves in Turbulent Pipe Flow," *Science*, **305**(5690), pp. 1594–1598.
- Matas, J.-P., Morris, J. F., and Guazzelli, E., 2003, "Transition to Turbulence in Particulate Pipe Flow," *Phys. Rev. Lett.*, **90**(1), p. 014501.
- Keefe, L., Moin, P., and Kim, J., 1992, "The Dimension of Attractors Underlying Periodic Turbulent Poiseuille Flow," *J. Fluid Mech.*, **242**, pp. 1–29.
- Karami, H., and Mowla, D., 2012, "Investigation of the Effects of Various Parameters on Pressure Drop Reduction in Crude Oil Pipelines by Drag Reducing Agents," *J. Non-Newton. Fluid Mech.*, **177**, pp. 37–45.
- Rotta J., 1956, "Experimenteller Beitrag zur Entstehung Turbulenter Strömung im Rohr," *Arch. Appl. Mech.*, **24**(4), pp. 258–281.
- Toms, B. A., 1948, "Some Observations on the Flow of Linear Polymer Solutions Through Straight Tubes at Large Reynolds Numbers," Proceedings of the 1st International Congress on Rheology, pp. 135–141.
- Virk, P., 1971, "Drag Reduction in Rough Pipes," *J. Fluid Mech.*, **45**(02), pp. 225–246.
- Virk, P., 1971, "An Elastic Sublayer Model for Drag Reduction by Dilute Solutions of Linear Macromolecules," *J. Fluid Mech.*, **45**(03), pp. 417–440.
- Virk, P. S., 1975, "Drag Reduction Fundamentals," *AIChE J.*, **21**(4), pp. 625–656.
- Virk, P. S., Merrill, E., Mickley, H., Smith, K., and Mollo-Christensen, E., 1967, "The Toms Phenomenon: Turbulent Pipe Flow of Dilute Polymer Solutions," *J. Fluid Mech.*, **30**(02), pp. 305–328.
- Warholic, M., Massah, H., and Hanratty, T., 1999, "Influence of Drag-Reducing Polymers on Turbulence: Effects of Reynolds Number, Concentration and Mixing," *Exp. Fluids*, **27**(5), pp. 461–472.
- Den Toonder, J., Hulsen, M., Kuiken, G., and Nieuwstadt, F., 1997, "Drag Reduction by Polymer Additives in a Turbulent Pipe Flow: Numerical and Laboratory Experiments," *J. Fluid Mech.*, **337**, pp. 193–231.
- Min, T., Yoo, J. Y., Choi, H., and Joseph, D. D., 2003, "Drag Reduction by Polymer Additives in a Turbulent Channel Flow," *J. Fluid Mech.*, **486**, pp. 213–238.
- Ptasinski, P., Nieuwstadt, F., Van Den Brule, B., and Hulsen, M., 2001, "Experiments in Turbulent Pipe Flow With Polymer Additives at Maximum Drag Reduction," *Flow, Turbul. Combust.*, **66**(2), pp. 159–182.
- Roy, A., and Larson, R. G., 2005, "A Mean Flow Model for Polymer and Fiber Turbulent Drag Reduction," *Appl. Rheol.*, **15**(6), pp. 370–389.
- White, C., Somandepalli, V., and Mungal, M., 2004, "The Turbulence Structure of Drag-Reduced Boundary Layer Flow," *Exp. Fluids*, **36**(1), pp. 62–69.
- Esmael, A., Nouar, C., Lefèvre, A., and Kabouya, N., 2010, "Transitional Flow of a Non-Newtonian Fluid in a Pipe: Experimental Evidence of Weak Turbulence Induced by Shear-Thinning Behavior," *Phys. Fluids*, **22**, p. 101701.

- [28] White, C. M., and Mungal, M. G., 2008, "Mechanics and Prediction of Turbulent Drag Reduction With Polymer Additives," *Annu. Rev. Fluid Mech.*, **40**, pp. 235–256.
- [29] Yang, S.-Q., and Dou, G., 2005, "Drag Reduction in a Flat-Plate Boundary Layer Flow by Polymer Additives," *Phys. Fluids*, **17**(6), p. 065104.
- [30] Yang, S.-Q., and Dou, G.-R., 2008, "Modeling of Viscoelastic Turbulent Flow in Channel and Pipe," *Phys. Fluids*, **20**(6), p. 065105.
- [31] Yang, S.-Q., 2009, "Drag Reduction in Turbulent Flow With Polymer Additives," *ASME J. Fluids Eng.*, **131**(5), p. 051301.
- [32] Yang, S.-Q., and Dou, G., 2010, "Turbulent Drag Reduction With Polymer Additive in Rough Pipes," *J. Fluid Mech.*, **642**, pp. 279–294.
- [33] Yang, S.-Q., and Ding, D., 2013, "Drag Reduction Induced by Polymer in Turbulent Pipe Flows," *Chem. Eng. Sci.*, **102**, pp. 200–208.
- [34] L'vov, V. S., Pomyalov, A., Procaccia, I., and Tiberkevich, V., 2004, "Drag Reduction by Polymers in Wall Bounded Turbulence," *Phys. Rev. Lett.*, **92**(24), p. 244503.
- [35] Emmons, H. W., 2012, "The Laminar-Turbulent Transition in a Boundary Layer-Part I," *J. Aeronaut. Sci.*, **18**(7), pp. 121–131.
- [36] Dou, G., 1996, "Basic Law in Mechanics of Turbulent Flows," *China Ocean Eng.*, **10**, pp. 1–45.
- [37] Spriggs, H. D., 1973, "Comments on Transition From Laminar to Turbulent Flow," *Ind. Eng. Chem. Fund.*, **12**(3), pp. 286–290.
- [38] Lumley, J. L., 1969, "Drag Reduction by Additives," *Annu. Rev. Fluid Mech.*, **1**(1), pp. 367–384.
- [39] Yang, S.-Q., Lim, S.-Y., and McCorquodale, J., 2005, "Investigation of Near Wall Velocity in 3-D Smooth Channel Flows," *J. Hydraul. Res.*, **43**(2), pp. 149–157.
- [40] Yang, S.-Q., 2010, "Conditionally Averaged Turbulent Structures in 2D Channel Flow," *Proc. ICE—Water Manage.*, **163**(2), pp. 79–88.
- [41] Presti, F., 2000, "Investigation of Transitional and Turbulent Pipe Flow of Non-Newtonian Fluids," Ph.D. thesis, University of Liverpool, Liverpool, UK.
- [42] Escudier, M., Presti, F., and Smith, S., 1998, "Drag Reduction in the Turbulent Pipe Flow of Polymers," *J. Non-Newton. Fluid Mech.*, **81**(3), pp. 197–213.
- [43] Narayanan, M. A. B., and Narayana, T., 1967, "Some Studies on Transition From Laminar to Turbulent Flow in a Two-Dimensional Channel," *ZAMP*, **18**(5), pp. 642–650.
- [44] Rao, G., 1974, "Mechanics of Transition in an Axisymmetric Laminar Boundary Layer on a Circular Cylinder," *ZAMP*, **25**(1), pp. 63–75.
- [45] Narasimha, R., 1985, "The Laminar-Turbulent Transition Zone in the Boundary Layer," *Prog. Aerospace Sci.*, **22**(1), pp. 29–80.
- [46] Wójs, K., 1993, "Laminar and Turbulent Flow of Dilute Polymer Solutions in Smooth and Rough Pipes," *J. Non-Newton. Fluid Mech.*, **48**(3), pp. 337–355.
- [47] Peixinho, J., Nouar, C., Desaubry, C., and Théron, B., 2005, "Laminar Transitional and Turbulent Flow of Yield Stress Fluid in a Pipe," *J. Non-Newton. Fluid Mech.*, **128**(2), pp. 172–184.
- [48] Dou, G., and Wang, G., 1988, "The Turbulence Structure of a Viscoelastic Fluid by Dilute Solution of Linear Macromolecules in the Interim State From Laminar Flow to Turbulent Flow," *J. Nanjing Hydraul. Res.*, **3**, pp. 1–14.
- [49] Jiménez, J., and Pinelli, A., 1999, "The Autonomous Cycle of Near-Wall Turbulence," *J. Fluid Mech.*, **389**, pp. 335–359.